Fluid Phase Equilibria 439 (2017) 18–23

Contents lists available at ScienceDirect

Fluid Phase Equilibria

journal homepage: www.elsevier.com/locate/fluid

Measurement and correlation of the interfacial tension for paraffin + CO_2 and (CO_2+N_2) mixture gas at elevated temperatures and pressures

Qiaoyan Shang [a, b], Shuqian Xia [b, *], GuanWei Cui [a], Bo Tang [a, **], Peisheng Ma [b]

[a] College of Chemistry, Chemical Engineering and Materials Science, Collaborative Innovation Center of Functionalized Probes for Chemical Imaging, Key Laboratory of Molecular and Nano Probes, Ministry of Education, Shandong Provincial Key Laboratory of Clean Production of Fine Chemicals, Shandong Normal University, Jinan 250014, China

[b] Key Laboratory for Green Chemical Technology of the State Education Ministry, Collaborative Innovation Center of Chemical Science and Engineering (Tianjin), School of Chemical Engineering and Technology, Tianjin University, Tianjin 300072, China

ARTICLE INFO

Article history:
Received 7 November 2016
Received in revised form
6 February 2017
Accepted 15 February 2017
Available online 20 February 2017

Keywords:
Enhanced oil recovery (EOR)
Interfacial tension (IFT)
Paraffin
Correlation

ABSTRACT

Interfacial tension (IFT) is crucial for characterizing the phase and interphase behavior in the enhanced oil recovery (EOR) process. CO_2 and N_2 are commonly used as injection gases in the EOR process. In this work, an experimental apparatus using the pendent drop method was adopted to measure IFTs for the EOR process with different injection gases, temperatures (40.0−120.0 °C) and pressures (0.22 −17.32 MPa). The relative Gibbs adsorption isotherm (Γ_{ij}) of a species *i* on species *j* were calculated by the experimental IFTs. Theoretically, new correlations were proposed to predict paraffin IFTs for pure CO_2 and mixture gas (CO_2 + N_2) injection. A total of 561 and 268 experimental IFTs were used to derive the correlations for pure CO_2 and mixture gas injection, respectively. The square of correlation coefficient (R^2), root mean square error (*RMSE*) and average absolute relative deviations (*AARD*) for pure CO_2 were 0.9884, 0.58 and 5.45%, respectively. For the mixture gas injection, the R^2, *RMSE* and *AARD* of the correlation were 0.9851, 0.57 and 4.47%, respectively.

1. Introduction

The gas injection technique of enhanced oil recovery (EOR) has recently been given increasing attention [1]. Various gases such as natural gas, carbon dioxide (CO_2) and nitrogen (N_2) have been injected into oil reservoirs to increase oil recovery [2]. Among these techniques, CO_2 flooding is known as the most effective method due to its high oil recovery and CO_2 sequestration to reduce greenhouse gas emission [3]. However, in some cases, asphaltene precipitation occurred during CO_2 flooding and caused severe problems such as relative permeability reduction and wettability alteration. To solve the issue of asphaltene precipitation, N_2 was injected into matured oil reservoirs to displace crude oil [4] due to its natural availability and chemical stability at low temperatures [2,5,6].

Generally, the gas injection process included miscible and immiscible displacements. The vanishing interfacial tension (VIT) technique was used to study the miscibility between crude oil and CO_2 systems. (The critical point for CO_2 was t_c = 31 °C and p_c = 7.4 MPa. The 'interfacial tension' term, not the 'surface tension' term, was used in this study because in that part of the study the CO_2 was under supercritical conditions. The density of supercritical CO_2 varied with pressure to values comparable to a liquid paraffin as studied in Haghbakhsh et al.'s work [7]) The VIT technique is based on the concept that interfacial tension (IFT) between crude oil and injection gas becomes zero when they are miscible [4,5,8–10].

The IFT was a key parameter for characterizing the phase and interphase behavior of the complex fluid systems [11,12]. An accurate IFT value is essential to evaluate the miscible injection process. The content of paraffins was higher than other alkanes in crude oil. Both experimental and theoretical work for the IFT of paraffins and injection gases have been conducted by many researchers. Until now, the most widely used method for measuring IFTs at elevated pressures was the pendant drop method

* Corresponding author.
** Corresponding author.
E-mail addresses: shuqianxia@tju.edu.cn (S. Xia), tangb@sdnu.edu.cn (B. Tang).

http://dx.doi.org/10.1016/j.fluid.2017.02.012
0378-3812/

[4,6,12–21]. Jaeger and Eggers [12] reported on the experimental IFTs of CO_2 + n-pentane/n-heptane systems. The IFTs decreased with pressure and the slope of IFTs versus pressures slightly diminished at elevated pressures for isothermal conditions. Zolghadr et al. [19] measured the IFTs of CO_2 + n-heptane/n-hexadecane with a temperature range of 40–120 °C and pressure range of 0.34–15.51 MPa. Cumicheo et al. [18] reported on the experimental isothermal densities and IFTs for three systems (CO_2 + n-dodecane/n-tridecane/n-tetradecane) at 71 °C under elevated pressures. Georgiadis et al. [14] measured IFTs of three systems (CO_2 + n-decane/n-dodecane/n-hexadecane) with a temperature range of 25–170 °C and pressures up to the critical points for each isotherm, and concluded that the IFT values showed a small increase with paraffin chain length. Mejía et al. [20] published the experimental IFTs of n-eicosane with a pressure range of 0.1–10.35 MPa at 50 °C. In addition, Tang et al. [21] measured the IFTs of N_2 + n-pentane/n-hexane/n-octane/n-decane with a pressure range 0.1–40 MPa at 40 °C. Garrido et al. [6] presented the experimental IFTs of N_2 + hexane with a temperature range of 30–60 °C and a pressure range 0.1–15.1 MPa. The trend of N_2 + paraffin IFTs with pressure or temperature was similar to CO_2 injection. However, the experimental IFTs of injection gas + paraffin, such as n-heptadecane, n-pentadecane, etc., are still insufficient for detailed design and operation of the EOR process, especially with (CO_2+N_2) mixture gas injection.

Theoretically, numerous studies have been performed to calculate IFT values, such as the parachor method [22,23], the density functional theory (DFT) [14] and the density gradient theory (DGT) [18,20,24]. The prediction ability of parachor method was limited because empirical density correlations were required in this method. Various intermolecular parameters were necessary to calculate IFT by the DFT method. An influence parameter is necessary in the DGT method, which was retrieved from one data point of experimental surface tension of the participating pure substances, and has large effects on the prediction abilities of DGT [24]. For the EOR process, the IFT was influenced by many factors such as the reservoir temperature, pressure, paraffin chain length and injection gas composition. So far, no explicit correlations of IFT values with all the factors for the EOR process were reported in literature. It is important to obtain accurate and general correlations for calculating IFTs.

An apparatus using the pendent drop method was designed and manufactured in our previous work. It was verified to be reliable and used to determine IFTs of simulated oil-pure/impure CO_2 [25]. The results showed that the IFT of simulated oil-impure CO_2 (a mixture of CO_2 with mole fraction 0.75 and N_2 with mole fraction 0.25) were higher than pure CO_2 injection. To further study the effect of N_2 on the EOR process, the same mixture gas composition of CO_2 and N_2 was used in this work. The IFTs for CO_2/(CO_2+N_2) mixture gas (1) + paraffin (2) (including n-nonane, n-undecane, n-tridecane, n-pentadecane and n-heptadecane) systems were measured at a wide range of pressures and temperatures. The relative Gibbs adsorption isotherm (Γ_{ij}) of a species i on species j were calculated by the experimental IFTs. Universal IFT correlations were proposed based on the IFT database, which includes CO_2 and (CO_2+N_2) mixture gas injection. The correlations relate IFT to reservoir temperature, pressure, paraffin chain length and N_2 mole fraction in injection gas.

2. Experiment

2.1. Materials

The purities and suppliers of five paraffins and two gases used in this study are listed in Table 1. The mixture gas used in this work was a mixture of CO_2 (mole fraction 0.75) and N_2 (mole fraction 0.25). All chemicals were used without any further purification treatment.

Table 1
Purities and suppliers of five paraffins and two gases used in this study[a].

Chemical	Supplier	Purity
n-Nonane	Tianjin Guangfu Technology Development Co., Ltd., China	0.990
n-Undecane	Tianjin Guangfu Technology Development Co., Ltd., China	0.990
n-Tridecane	Tianjin Guangfu Technology Development Co., Ltd., China	0.985
n-Pentadecane	Shanghai Aladdin Industrial Co., Ltd., China	0.990
n-Heptadecane	Tianjin Heowns Biochemical Technology Co., Ltd., China	0.990
Carbon Dioxide	Tianjin Liufang Industrial gases co., Ltd., China	0.999
Nitrogen	Tianjin Liufang Industrial gases co., Ltd., China	0.999

[a] The purity was mole fraction.

2.2. IFT measurement

The pendent drop method was used to measure the equilibrium IFTs. The schematic diagram of the apparatus and experimental procedure was shown in our previous work [25]. This apparatus includes three major sections: a high-pressure view cell (HPVC), syringe pump (SP) and programmable syringe pump (PSP). The accuracy of the HPVC temperature was ±0.1 °C. The relative uncertainty of the pressure transducer (CYB-20S, Beijing Westzh M&E Technology Ltd., China) was 0.1% with the full scale up to 40 MPa. The densities of the two phases at the equilibrium condition were necessary for the pendent drop method. The densities of pure CO_2 were obtained by the Benedict Webb Rubin Starling equation of state (BWRS EOS) [26]. The BWRS EOS and mixing rules were used to calculate the density of (CO_2 + N_2) mixture gas and shown in the Supporting Information Appendix. Liquid densities were calculated by the National Institute of Standards and Technology [27]. Referring to the literature [14,28], the IFTs were based on bulk phase densities of the pure CO_2, (CO_2 + N_2) mixture gas and paraffin rather than on the actual density of the mixture (paraffins + CO_2 or paraffins + (CO_2+N_2) mixture gas). The selected plane method were used to obtain the IFT values. The theory and equations can be seen in Andreas et al.'s work [29]. The IFT measurement process was repeated for at least three times to ensure satisfactory repeatability.

The uncertainties of γ were affected by the temperature, pressure, density difference, the experimental reproducibility of γ itself and its standard uncertainties. To quantify these effects in the relative uncertainty (u_r) of γ, the following relationship [30] was used:

$$u_r^2(\gamma) = \left[\frac{1}{\gamma}\left(\frac{\partial\gamma}{\partial p}\right)_t \delta p\right]^2 + \left[\frac{\delta\Delta\rho}{\Delta\rho}\right]^2 + \left[\frac{\sigma(\gamma)}{\gamma}\right]^2 \quad (1)$$

where δp and $\delta\Delta\rho$ correspond to the standard uncertainties in pressure and density, respectively. $\sigma(\gamma)$ is the standard deviation of γ which, together with the maximum value of partial derivatives of γ in p, have directly been estimated from experimental data. The average u_r was 0.67% for the binary systems in this work, which was calculated from the uncertainties of temperature, pressure, and density difference.

A total of 215 IFTs for CO_2 (1) + paraffin (2) (including n-nonane, n-undecane, n-tridecane, n-pentadecane and n-heptadecane) systems and 202 IFTs for (CO_2+N_2) mixture gas (1) + paraffin (2)

systems were measured with the temperature (40.0–120.0 °C) and pressure (0.22–17.32 MPa). All experimental IFT data are shown in Tables S1 and S2.

3. Empirical numerical correlation

3.1. Factors influencing the injection gas + paraffin IFTs

Fig. 1 shows the IFTs as a function of pressure for injection gas (1) + n-heptadecene (2) at different temperatures. For the pure CO_2 injection, it can be seen that the experimental IFTs decreased with pressure and approximated the straight lines in the studied ranges. The slope of IFT versus pressure slightly decreased at elevated temperatures. In addition, the IFT decreased with temperature at lower pressures (lower than (4.5–5.5) MPa for CO_2 (1) + n-heptadecene (2) systems) and increased with temperature at higher pressures. The IFT exhibits the weakest dependence on temperature at the crossover-pressure. These results indicate that CO_2 injection is recommended at lower temperatures above crossover-pressures and higher temperatures below crossover-pressures for maintaining better conditions. The IFTs of CO_2 (1) + paraffins (2) as a function of pressure are shown in Fig. 2. The IFTs showed a small increase with paraffin chain length when the temperature and pressure was kept constant. The trend of paraffin IFTs with pressure or temperature was similar to the conclusions in literature [12,14,19]. The N_2 in the injection gas caused higher IFTs than pure CO_2 injection at pressures higher than approximately 6.5 MPa as shown in Fig. 1. The IFT exhibits the weakest dependence on N_2 when the pressure was less than approximately 6.5 MPa. A similar trend with other paraffins is shown in Figs. S1–S4.

3.2. Developing the injection gas + paraffin IFTs models

As mentioned above, the injection gas + paraffin IFTs were strongly related to reservoir temperature, pressure, paraffin chain length and N_2 mole fraction in the mixture gas. It is necessary to consider these influenced factors when developing IFT correlations. In this work, the IFTs of paraffin + CO_2 system were presented as a function of reservoir temperature, pressure and paraffin chain length. The IFTs of paraffin + (CO_2+N_2) mixture gas system were correlated with reservoir temperature, pressure, N_2 mole fraction and paraffin chain length. Equations (2) and (3) were proposed and

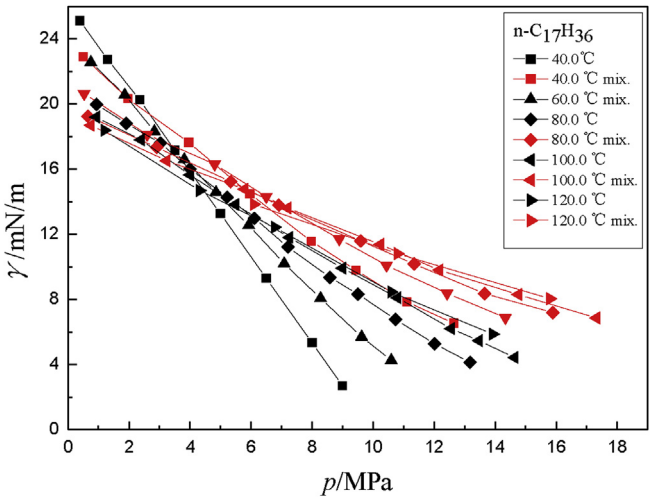

Fig. 1. The comparisons of n-heptadecane IFTs for pure CO_2 and mixture gas (CO_2 0.75, N_2 0.25) injection.

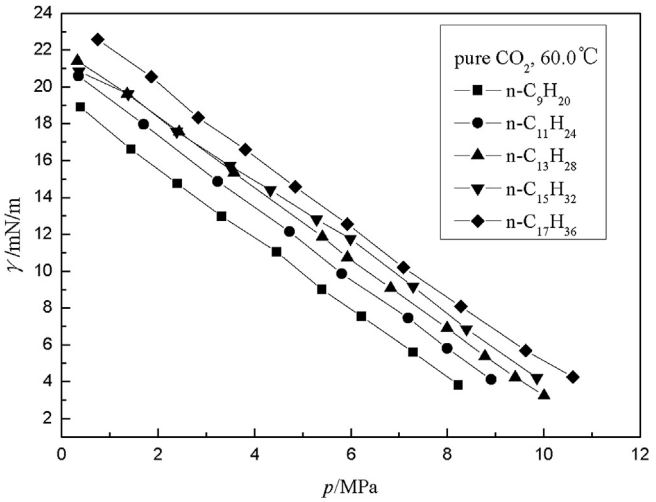

Fig. 2. The IFTs of CO_2 (1) + paraffin (2) as a function of pressure at 60.0 °C.

utilized to calculate paraffin IFTs for pure CO_2 and (CO_2+N_2) mixture gas injection, respectively.

$$\gamma = \left(a \cdot t^b + c \cdot t\right) \cdot p \cdot N^d + e \cdot p \cdot N^d + f \cdot t^g + h \cdot N^d \tag{2}$$

$$\gamma = \left(a \cdot t^b + c \cdot t\right) \cdot p \cdot \left(1 - x_{N_2}\right) + d \cdot t \cdot N^e + f \cdot p^g + i \cdot p \cdot x_{N_2} + h \cdot N^e \tag{3}$$

where γ is IFT in mN/m, t is reservoir temperature in °C, p is pressure in MPa, N is carbon number in paraffin, x_{N_2} is N_2 mole fraction in mixture gas. a, b, c, d, e, f, g, h and i are empirical coefficients.

The objective function OF is expressed as follows:

$$OF = \min \sum \left(\gamma_{exp.} - \gamma_{cal.}\right)^2 \tag{4}$$

where $\gamma_{exp.}$ and $\gamma_{cal.}$ are the experimental and calculated IFTs, respectively. The empirical coefficients of equations were obtained by the least square method.

The statistical parameters included square of correlation coefficient (R^2), root mean square error ($RMSE$) and average absolute relative deviations ($AARD$) were used to evaluate the accuracy of the new models.

$$RMSE = \sqrt{\frac{\sum_{i=1}^{n}\left(\gamma_{exp.} - \gamma_{cal.}\right)^2}{n}} \tag{5}$$

$$AARD\% = \frac{\sum_{i=1}^{n}\frac{\left|\gamma_{exp.} - \gamma_{cal.}\right|}{\gamma_{cal.}} \times 100}{n} \tag{6}$$

For pure CO_2 systems, a total of 561 data points including 215 IFTs in this work and 346 IFTs from literature [12,14,18–20] were used to correlate Equation (2). The studied ranges of temperature and pressure were 24.7–169.9 °C and 0.1–19.0 MPa, respectively. For mixture gas systems, 268 data points including 202 IFTs in this work and 66 IFTs from literature [6,21] were adopted to correlate Equation (3). The studied ranges of temperature and pressure were 30.0–120.0 °C and 0.1–40.2 MPa, respectively. The N_2 mole fraction was from 0.25 to 1. The correlations was reasonable and adopted in the studied range. The IFT database is given in the Supporting

Information. The database includes the carbon number in paraffin from 5 to 20. The regressed coefficients of Equations (2) and (3) are listed in Table 2.

4. Results and discussion

4.1. The relative Gibbs adsorption isotherm

The experimental IFTs can be used to predict the relative Gibbs adsorption isotherm (Γ_{ij}) of a species *i* on species *j*, which was used to explain the adsorption of CO_2 in paraffin. According to Masterton et al.'s [31] and Cumicheo et al.'s [18] work, for a gas–liquid system with changing pressure, the Γ_{ij} equation was shown by the following expression:

$$\Gamma_{12} = -\frac{\rho_1}{M_1}\left(\frac{\partial\gamma}{\partial p}\right)_t \quad (7)$$

where the slope $(\partial\gamma/\partial p)_t$ is obtained from experimental values of $\gamma \sim p$. ρ_1 and M_1 are the density and molecular weight of the injection gas, respectively. ρ_1 was obtained by the BWRS EOS in the work.

The adsorption of injection gases (1) in paraffin (2) was approximately quantified by the relative Gibbs adsorption isotherm (Γ_{12}). The Γ_{12} was calculated by Equation (7), and the detailed results were shown in Supporting Information. The comparisons of Γ_{12} for pure CO_2/mixture gas (1) + n-heptadecane (2) as a function of pressure (p) at different temperatures are shown in Fig. 3. Γ_{12} increased with pressure and decreased with temperature for pure CO_2 injection. For the mixture gas, the Γ_{12} was lower than the values of pure CO_2 at the same pressure and temperature. The similar trend of other systems are shown in Figs. S5–S8. As mentioned above, we can see that the trends of Γ_{12} with changing temperature and pressure were opposite the trends of the IFTs.

4.2. The empirical numerical correlation

To test the reliability of the new correlations, the IFTs calculated by the new correlations were compared with the experimental IFTs. The detailed calculated results are presented in the Supporting Information.

The overall calculation results of the correlations for pure CO_2 and mixture gas are shown in Tables 3 and 4, respectively. For pure CO_2 systems, the overall R^2, *RMSE* and *AARD* were 0.9884, 0.58 and 5.45%, respectively, as listed in Table 3. Fig. 4 shows the comparison between the experimental IFTs and the calculated values from Equation (2). It can be seen that the majority of points are located in the vicinity of the bisection in Fig. 4. For the mixture gas systems, Table 4 lists the detailed calculation results of Equation (3), including R^2 of 0.9851, *RMSE* of 0.57 and *AARD* of 4.47%. The scatter plot of the experimental IFTs versus the calculated IFTs from Equation (3) is shown in Fig. 5. Fig. 5 and Table 4 demonstrate that Equation (3) can calculate the mixture gas + paraffin IFTs precisely. In other words, it is reliable for calculating IFTs of paraffin + CO_2/(CO_2+N_2) mixture gas using the new correlations.

To further examine and validate the accuracy of the new correlations, the methods of Leave One Out Cross Validation (LOOCV) and external validation were used to investigate the applicability of the new correlations.

Table 2
The values of coefficients of Equations (2) and (3).

Equation (2)		Equation (3)	
Coefficient	Value	Coefficient	Value
a	−15.8	*a*	−10.8
b	−0.305	*b*	−0.520
c	−0.00490	*c*	0.00130
d	0.177	*d*	−0.529
e	3.68	*e*	−0.915
f	−18.0	*f*	28.0
g	0.179	*g*	−0.0248
h	37.3	*h*	−44.4
i		*i*	−0.279

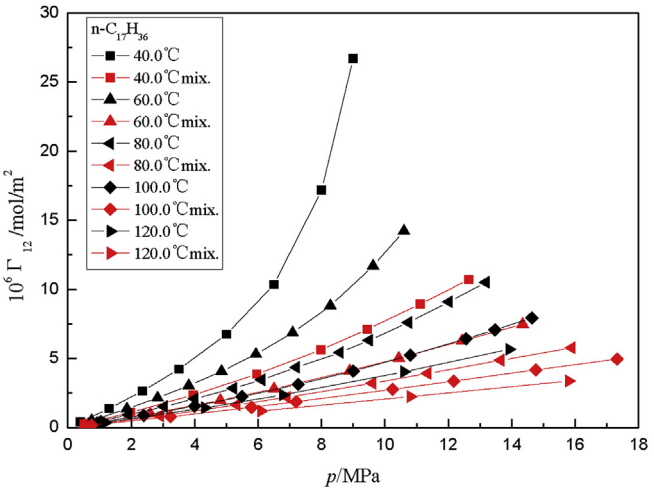

Fig. 3. The comparisons of relative Gibbs adsorption isotherm for pure CO_2/mixture gas (1) + n-heptadecane (2), Γ_{12}, as a function of pressure (p) at different temperatures.

4.2.1. Leave One Out Cross Validation (LOOCV)

LOOCV is the method that leaves out a set of samples for each test, while the other samples form a training set. If there are k samples, k times training and k times testing are required. The samples are used adequately in LOOCV. The prediction abilities of Equations (2) and (3) were tested by LOOCV and are listed in Tables 3 and 4. For pure CO_2 systems, the R^2 (0.9883) and *RMSE* (0.57) for LOOCV were almost the same as in Equation (2). The *AARD* (5.10%) for LOOCV is slightly less than that (5.45%) of Equation (2). For mixture gas systems, the R^2 (0.9859), *RMSE* (0.55) and *AARD* (4.46%) for LOOCV were nearly the same as in Equation (3). From the above, the new models are feasible for predicting IFTs of paraffin + CO_2/(CO_2+N_2) mixture gas.

Table 3
The results of the Equation (2) prediction ability test by LOOCV and external validation.

Status	Data points	R^2	*RMSE*	*AARD%*
Model	561	0.9884	0.58	5.45
LOOCV	561	0.9883	0.57	5.10
Training	421	0.9880	0.58	5.44
Testing	140	0.9894	0.59	5.15

Table 4
The results of the Equation (3) prediction ability test by LOOCV and external validation.

Status	Data points	R^2	*RMSE*	*AARD%*
Model	268	0.9851	0.57	4.47
LOOCV	268	0.9859	0.55	4.46
Training	203	0.9851	0.57	4.47
Testing	65	0.9849	0.58	4.50

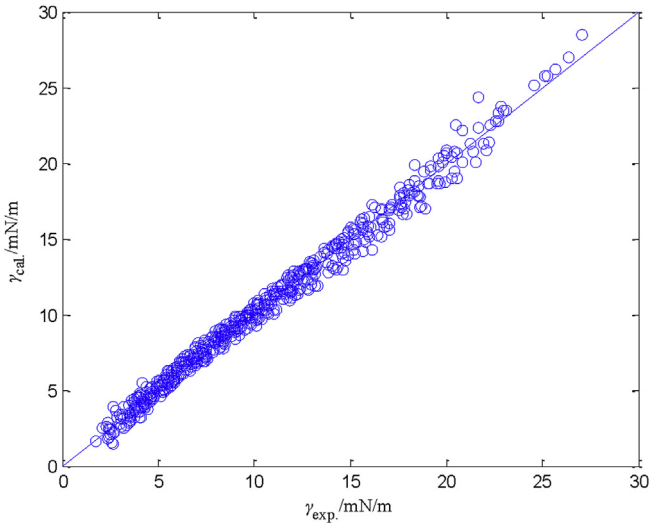

Fig. 4. The comparisons between the experimental IFTs and predicted values by Equation (2) for paraffin + CO_2 systems.

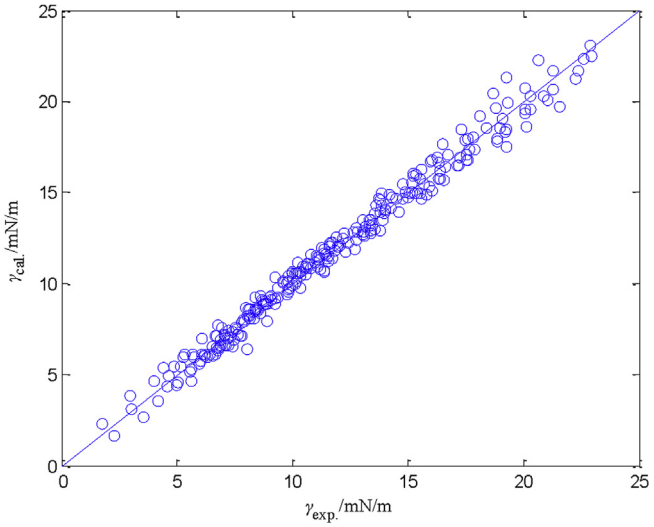

Fig. 5. The comparisons between the experimental IFTs and predicted values by Equation (3) for paraffin + mixture gas systems.

4.2.2. External validation

In this method, the database was randomly divided into a training set and a testing set. The correlation was regressed by the training set with the same parameters. For pure CO_2 systems, the database was randomly divided into a training set (421) and a testing set (140). The correlation was regressed by the training set with the same parameters used in Equation (2). The IFTs of the testing set were predicted by this correlation. The statistical parameters of the training and testing set are listed in Table 3. The R^2, *RMSE* and *AARD* in the training set were approximated by those of all data points. For mixture gas systems, the database was also randomly divided into a training set (203) and a testing set (65). The correlation was obtained by the training set with the same parameters used in Equation (3) and used to estimate the IFTs of the testing set. The detailed calculated results of the training and testing set are given in Table 4. The R^2, *RMSE* and *AARD* in the training set were as good as those containing all data points. It was thus proven that the correlation can accurately estimate paraffin + mixture gas IFTs. The overall results showed that new correlations have great predictive abilities.

5. Conclusions

In this work, the IFTs of the binary systems pure CO_2/(CO_2+N_2) mixture gas + paraffin (n-nonane/n-undecane/n-tridecane/n-pentadecane/n-heptadecane) were measured with the temperature (40.0–120.0 °C) and pressure (0.22–17.32 MPa). The relative Gibbs adsorption isotherm (Γ_{12}) were calculated by the experimental IFTs. Γ_{12} increased with pressure and decreased with temperature. For the mixture gas, the Γ_{12} were lower than the values of pure CO_2 at same pressure and temperature. The IFTs were influenced by reservoir temperature, pressure, paraffin chain length and N_2 mole fraction. The new correlations were proposed to estimate paraffin IFTs for CO_2 and (CO_2+N_2) mixture gas injection according to these influenced factors. A total of 561 and 268 experimental IFT data for CO_2 + paraffin and (CO_2+N_2) mixture gas + paraffin from this work and literature were used to obtain the correlations, respectively. The R^2, *RMSE* and *AARD* for the CO_2 + paraffin IFT correlation were 0.9884, 0.58 and 5.45%, respectively. The R^2, *RMSE* and *AARD* for the mixture gas injection correlation were 0.9851, 0.57 and 4.47%, respectively. LOOCV and external validation methods were used to examine the reliability and accuracy of the new correlations. The results determined that the new correlations can precisely estimate paraffin IFTs for pure CO_2 and mixture gas injection.

Acknowledgments

This research was supported by the National Key Research and Development Plan (No. 2016YFB00600804).

Appendix A. Supplementary data

Supplementary data related to this article can be found at http://dx.doi.org/10.1016/j.fluid.2017.02.012.

References

[1] G. Chen, X. Wang, Z. Liang, R. Gao, T. Sema, P. Luo, F. Zeng, P. Tontiwachwuthikul, Simulation of CO_2-oil minimum miscibility pressure (MMP) for CO_2 enhanced oil recovery (EOR) using neural networks, Energy Proced. 37 (2013) 6877–6884.
[2] A. Hemmati-Sarapardeh, S. Ayatollahi, A. Zolghadr, M.-H. Ghazanfari, M. Masihi, Experimental determination of equilibrium interfacial tension for nitrogen-crude oil during the gas injection process: the role of temperature, pressure, and composition, J. Chem. Eng. Data 59 (2014) 3461–3469.
[3] X. Wang, Y. Gu, Oil recovery and permeability reduction of a tight sandstone reservoir in immiscible and miscible CO_2 flooding processes, Ind. Eng. Chem. Res. 50 (2011) 2388–2399.
[4] A. Hemmati-Sarapardeh, S. Ayatollahi, M.-H. Ghazanfari, M. Masihi, Experimental determination of interfacial tension and miscibility of the CO_2-crude oil system; temperature, pressure, and composition effects, J. Chem. Eng. Data 59 (2014) 61–69.
[5] A. Zolghadr, M. Riazi, M. Escrochi, S. Ayatollahi, Investigating the effects of temperature, pressure, and paraffin groups on the N_2 miscibility in hydrocarbon liquids using the interfacial tension measurement method, Ind. Eng. Chem. Res. 52 (2013) 9851–9857.
[6] J.M. Garrido, L. Cifuentes, M. Cartes, H. Segura, A. Mejía, High-pressure interfacial tensions for nitrogen+ethanol, or hexane or 2-methoxy-2-methylbutane: a comparison between experimental tensiometry and Monte Carlo simulations, J. Supercrit. Fluids 89 (2014) 78–88.
[7] R. Haghbakhsh, H. Hayer, M. Saidi, S. Keshtkari, F. Esmaeilzadeh, Density estimation of pure carbon dioxide at supercritical region and estimation solubility of solid compounds in supercritical carbon dioxide: correlation approach based on sensitivity analysis, Fluid Phase Equilib. 342 (2013) 31–41.
[8] M. Nobakht, S. Moghadam, Y. Gu, Determination of CO_2 minimum miscibility pressure from measured and predicted equilibrium interfacial tensions, Ind. Eng. Chem. Res. 47 (2008) 8918–8925.
[9] A. Zolghadr, M. Escrochi, S. Ayatollahi, Temperature and composition effect on CO_2 miscibility by interfacial tension measurement, J. Chem. Eng. Data 58 (2013) 1168–1175.
[10] D.W. Green, G.P. Willhite, Enhanced oil recovery, in: L. Henry (Ed.), Doherty

Memorial Fund of AIME, Society of Petroleum Engineers, Richardson, Texas, 1998.
[11] O.G. Nino-Amezquita, S. Enders, P.T. Jaeger, R. Eggers, Measurement and prediction of interfacial tension of binary mixtures, Ind. Eng. Chem. Res. 49 (2009) 592–601.
[12] P.T. Jaeger, R. Eggers, Interfacial properties at elevated pressures in reservoir systems containing compressed or supercritical carbon dioxide, J. Supercrit. Fluids 66 (2012) 80–85.
[13] J.J.C. Hsu, N. Nagarajan, R.L. Robinson, Equilibrium phase compositions, phase densities, and interfacial tensions for carbon dioxide + hydrocarbon systems. 1. Carbon dioxide + n-butane, J. Chem. Eng. Data 30 (1985) 485–491.
[14] A. Georgiadis, F. Llovell, A. Bismarck, F.J. Blas, A. Galindo, G.C. Maitland, J.P.M. Trusler, G. Jackson, Interfacial tension measurements and modelling of (carbon dioxide + n-alkane) and (carbon dioxide + water) binary mixtures at elevated pressures and temperatures, J. Supercrit. Fluids 55 (2010) 743–754.
[15] S. Banerjee, J.M. Kleijn, M.A.C. Stuart, F.A.M. Leermakers, A liquid CO_2-compatible hydrocarbon surfactant: experiment and modelling, PCCP 15 (2013) 19879–19892.
[16] A. Hebach, A. Oberhof, N. Dahmen, A. Kögel, H. Ederer, E. Dinjus, Interfacial tension at elevated pressures measurements and correlations in the water + carbon dioxide system, J. Chem. Eng. Data 47 (2002) 1540–1546.
[17] P. Chiquet, J.-L. Daridon, D. Broseta, S. Thibeau, CO_2/water interfacial tensions under pressure and temperature conditions of CO_2 geological storage, Energy Convers. Manag. 48 (2007) 736–744.
[18] C. Cumicheo, M. Cartes, H. Segura, E.A. Müller, A. Mejía, High-pressure densities and interfacial tensions of binary systems containing carbon dioxide+n-alkanes: (n-Dodecane, n-tridecane, n-tetradecane), Fluid Phase Equilib. 380 (2014) 82–92.
[19] A. Zolghadr, M. Escrochi, S. Ayatollahi, Temperature and composition effect on CO_2 miscibility by interfacial tension measurement, J. Chem. Eng. Data 58 (2013) 1168–1175.
[20] A. Mejía, M. Cartes, H. Segura, E.A. Müller, Use of equations of state and coarse grained simulations to complement experiments: describing the interfacial properties of carbon dioxide + decane and carbon dioxide + eicosane mixtures, J. Chem. Eng. Data 59 (2014) 2928–2941.
[21] T. Jianhua, J. Satherley, D. Schiffrin, Density and interfacial tension of nitrogen-hydrocarbon systems at elevated pressures, Chin. J. Chem. Eng. 1 (1993) 223–231.
[22] S.C. Ayirala, D.N. Rao, A new mechanistic Parachor model to predict dynamic interfacial tension and miscibility in multicomponent hydrocarbon systems, J. Colloid Interface Sci. 299 (2006) 321–331.
[23] H. Li, D. Yang, P. Tontiwachwuthikul, Experimental and theoretical determination of equilibrium interfacial tension for the solvent(s)-CO_2-heavy oil systems, Energy Fuels 26 (2012) 1776–1786.
[24] H. Lin, Y.-Y. Duan, Q. Min, Gradient theory modeling of surface tension for pure fluids and binary mixtures, Fluid Phase Equilib. 254 (2007) 75–90.
[25] Q. Shang, S. Xia, M. Shen, P. Ma, Experiment and correlations for CO_2–oil minimum miscibility pressure in pure and impure CO_2 streams, RSC Adv. 4 (2014) 63824–63830.
[26] Y. Wu, B. Chen, The application of BWRS equation in calculating the thermophysical properties of natural gas, Oil Gas Storage Transp. 22 (2003) 16.
[27] M. Huber, NIST Thermophysical Properties of Hydrocarbon Mixtures Database (SUPERTRAPP), 2003, p. 4. NIST Standard Reference Database.
[28] A. Georgiadis, G. Maitland, J.P.M. Trusler, A. Bismarck, Interfacial tension measurements of the (H_2O + CO_2) system at elevated pressures and temperatures, J. Chem. Eng. Data 55 (2010) 4168–4175.
[29] J.M. Andreas, E.A. Hauser, W.B. Tucker, Boundary tension by pendant drops 1, J. Phys. Chem. 42 (1937) 1001–1019.
[30] B.N. Taylor, C.E. Kuyatt, Guidelines for Evaluating and Expressing the Uncertainty of NIST Measurement Results, US Department of Commerce, Technology Administration, National Institute of Standards and Technology Gaithersburg, MD, 1994.
[31] W. Masterton, J. Bianchi, E. Slowinski Jr., Surface tension and adsorption in gas—liquid systems at moderate pressures 1, J. Phys. Chem. 67 (1963) 615–618.